Middle East Technical University

Electrical and Electronics Engineering

EE463: Static Power Conversion

Term Final Project Report

CONVERTEROĞULLARI TİC. A.Ş.

İbrahim Yaman 2576288

Esma Duman 2604932

Muhammed Raşid Gökcen 2443091

Table of Contents

Introduction

For our EE463 course term project, we designed, implemented, and tested a DC motor drive module. The final product rectifies the grid voltage and steps it down to a lower level to feed to a 2 kW DC motor.

This report explains all the design decisions we made, including topology and component selection, simulations, and loss calculations to correctly address and find a resolution to our task, as well as our hardware test results and a discussion of the strengths and weaknesses of the final product.

Project Specifications

The project requires the implementation of a controlled rectifier to drive a DC motor. The input will either be 3 or single phase AC grid, adjustable through a variac. The current ripple is supposed to be greater than 1 kHz. Also, a maximum of only 2 power sources (including the variac) can be used in addition to the field excitation.

The aforementioned DC motor will be coupled to a generator, and the motor specifications are as follows:

- 1500 rpm
- Voltage/Current rating: 220 V/23.4 A
- Armature Winding: 0.8 Ω, 12.5 mH
- Shunt Winding: 210 Ω, 23 H
- Interpoles Winding: 0.27 Ω, 12 mH

Design Decisions

Topology Selection

To design an appropriate module, we devised and evaluated different topologies in terms of effectiveness, feasibility, and cost. We analysed and compared the following topologies, the advantages and disadvantages of which can be seen in Tables 1-3:

- 3-phase thyristor rectifier
- 3-phase diode rectifier and buck converter
- 1-phase diode rectifier and buck converter

Table 1: Advantages & Disadvantages of 3-Phase Thyristor Rectifier Topology

3-Phase Thyristor Rectifier	
Advantages	**Disadvantages**
Suitable for high-power applications	High current ripple
Simple controller	Poor grid power factor
Low cost	Pulsating torque on the DC motor

Table 2: Advantages & Disadvantages of 3-Phase Diode Rectifier & Buck Converter Topology.

3-Phase Diode Rectifier & Buck Converter	
Advantages	**Disadvantages**
Suitable for medium to high power applications	Complex drive
Precise control with PWM	Moderate cost
Small motor current ripple	
Good grid power factor (DPF =1)	
Smooth DC motor torque	
Low output voltage ripple	

Table 3: Advantages & Disadvantages of 1-Phase Diode Rectifier & Buck Converter Topology.

1-Phase Diode Rectifier & Buck Converter	
Advantages	**Disadvantages**
Suitable for low to medium power applications	Complex drive (Simpler than 3-phase)
Precise control with PWM	Poor grid power factor (Low PF)
Small motor current ripple	
Smooth DC motor torque.	
Low output voltage ripple	
Low cost	

After analysing the 3 options, we decided to carry out a single-phase diode rectifier and buck converter topology considering its suitable power rating, low cost, low pulsating torque, and simple implementation.

The rest of this section will discuss how each portion of the motor driver, these being the rectifier, buck converter, and controller, was designed and why specific decisions were made.

Diode Rectifier Design

As discussed previously, the input of the driver firstly passes through a single-phase diode rectifier to then be leveled down. The model of the implemented design can be seen in Figure 1 below.

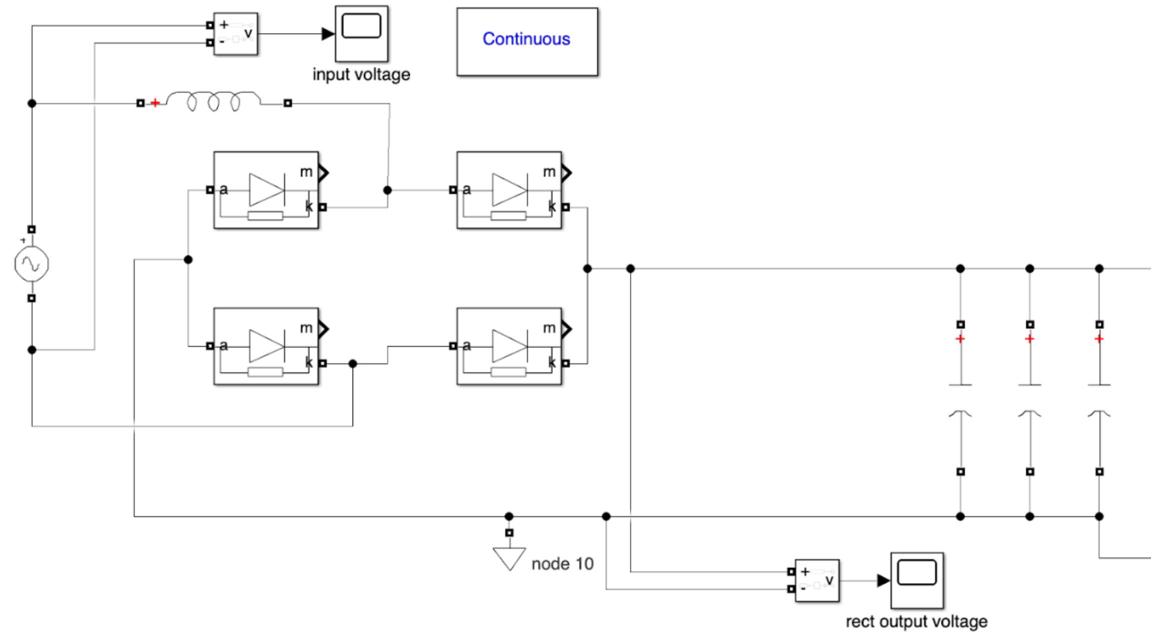

Figure 1: Rectifier Design

As can be observed, the structure simply consists of 4 diodes for full-wave rectification of a single phase, and output capacitors. The inductor at the input is simply placed to model the line inductance and is not a part of our actual design. In place of the four diodes, a rectifier bridge is used in the final product.

Two of the three output capacitors are large ones rated at 470µ F for output voltage ripple reduction, whereas the last one is a smaller capacitor of 10n F merely placed to reduce the overall ESR of the bundle.

Further specifications on both the bridge and capacitors are discussed in the section entitled 'Component Selection.'

The approximate output voltage of the single-phase rectifier can be calculated as follows:

$$I_{load} = \frac{2kW}{220V} = 9.1A$$

$$V_{ripple} \cong \frac{I_{load}}{2 * f * C_{out}} = \frac{9.1A}{2 * (50Hz) * (2.470\mu H)} \cong 96.8V$$

$$V_{rectified,avg} = V_{peak} - 2V_D - \frac{V_{ripple}}{2} = 230\sqrt{2}V - 2 * 0.7V - \frac{96.8V}{2} = 275.47V$$

Buck Converter Design

The leveling down of the grid voltage is done using a buck converter connected between the rectifier output and the load input. The original design of the converter complied with the usual buck topology, as can be seen in Figure 2 below.

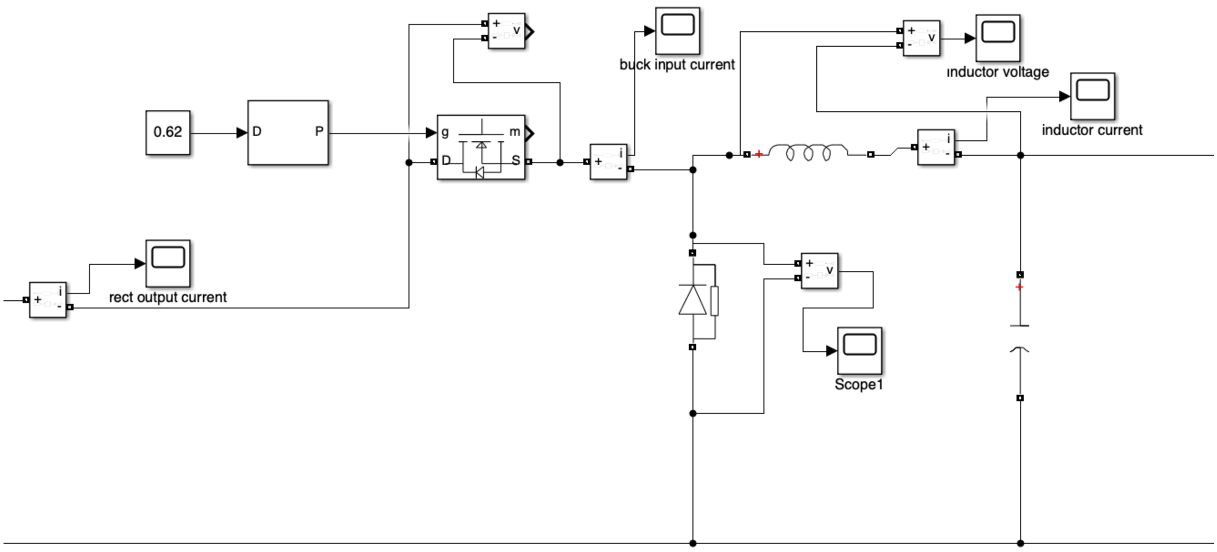

Figure 2: Original Buck Converter Design

Just as the general buck topology, this design used a power MOSFET as the switching element, a power diode for single-routed conduction, and an LC pair for smoothing of the output voltage and current. After analysis, however, we decided to remove the LC filter from the hardware design as the load is a motor, which is highly inductive itself. This leaves us no need to pre-smoothify the waveforms before feeding them to the load, also saving us the trouble of finding an inductor suitable for our application, which would have been excessively large.

As we decided not to place an extra inductor or a capacitor, we could set our switching frequency low, at 1 kHz, without worrying about the sizes of the aforementioned components. With a duty cycle of 0.8, the output voltage of the module, for an input of 275.5 V as rectified by the previous circuitry, will be approximately Vout = D · Vin = 0.8 ·275.5 ≈ 220.4 V, as required.

The model of the overall circuit, excluding the controller, can be seen below in Figure 3:

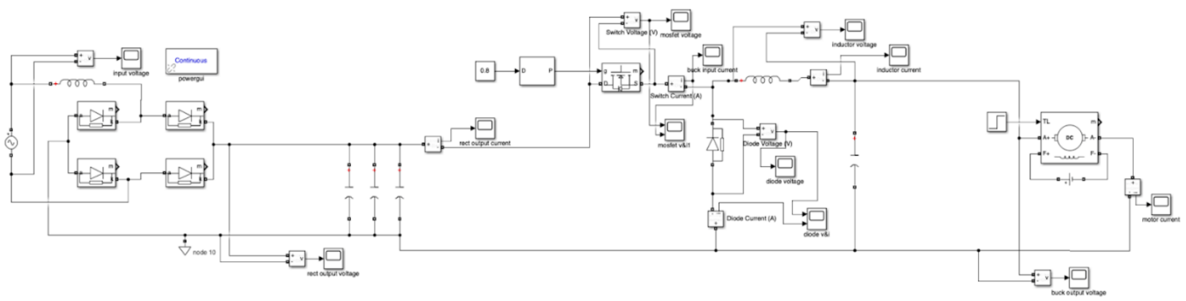

Figure 3: Overall Design

Controller Design

Simulation Results

Before hardware implementation, we completed and compared various simulations for each part of the design and the overall circuit. In this section, we will discuss the simulation results of our final models.

To start with, our full-wave diode rectifier design with ripple capacitors, its output voltage when loaded and connected to the grid (230 Vrms) can be seen in Figure 4 below.

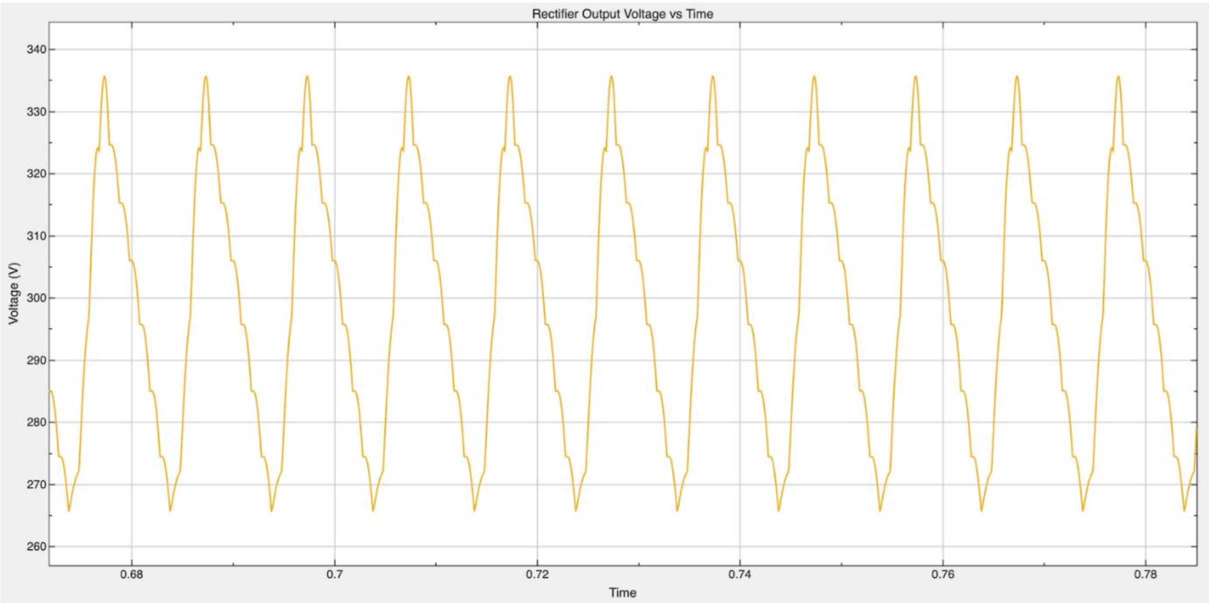

Figure 4: Rectifier Output Voltage Waveform

As can be observed from the figure, the obtained output ripple is in fact only around 70 V, smaller than the previously calculated amount. The reason for this is partially that the formula used does not account for the actual discharging time of the capacitor, and also that the simulation accounts for inductive components, such as the line inductance, which lowers the expected ripple amount. This is beneficial for us as a lower ripple introduces less parasitics and a signal closer to DC.

Moving on to the buck converter, this portion is designed to regulate and step down the DC output of the rectifier to feed to the DC motor. Its output voltage can be seen in Figure 5 below.

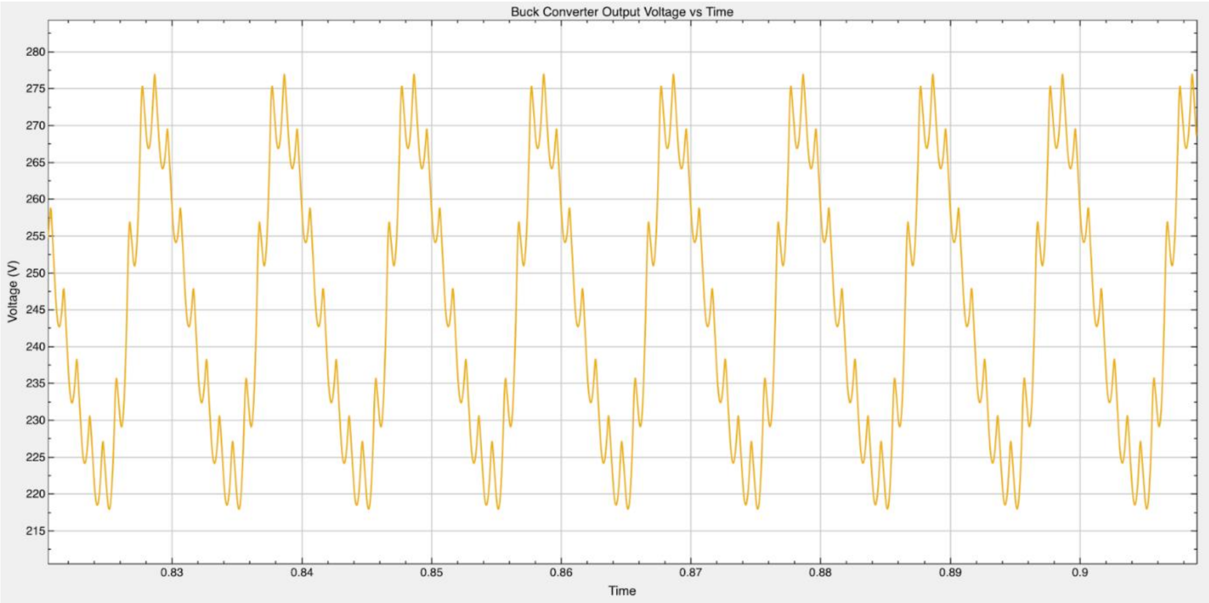

Figure 5: Buck Converter Output Voltage Ripple

Analysing the graph, it can be said that the voltage level fittingly decreases as intended, to around 240 V, with a slightly decreased ripple of approximately 60 V. The output voltage being slightly higher than the rated 220 V is not a serious issue, as it will allow for a lower input voltage for the purposeful output.

The switching current and voltage across the MOSFET are shown in Figure 6 below.

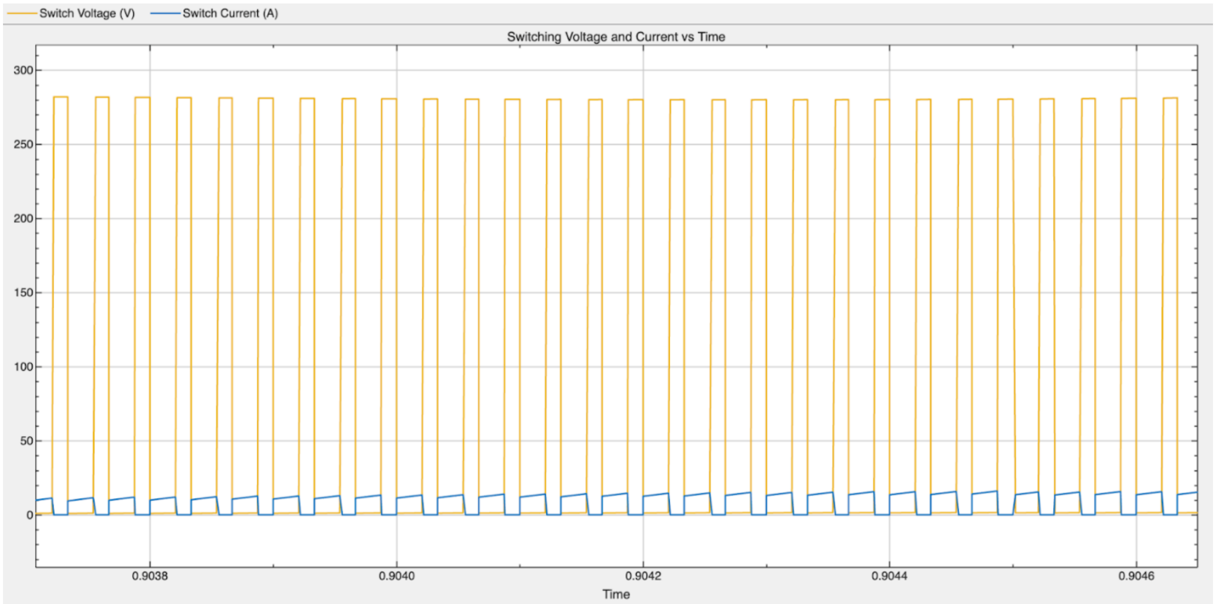

Figure 6: Switch Voltage & Current

We can see from this graph that when the MOSFET successfully blocks the voltage, its current is 0, and when the switch is conducting, the current starts flowing, following an almost-square waveform. The blocking voltage is fittingly around 280 V, whereas the turn-on resistance is almost negligible. The pulsating voltage waveform with sharp edges displays the correct functioning of the PWM signal.

Below in Figure 7 are the diode voltage and current waveforms.

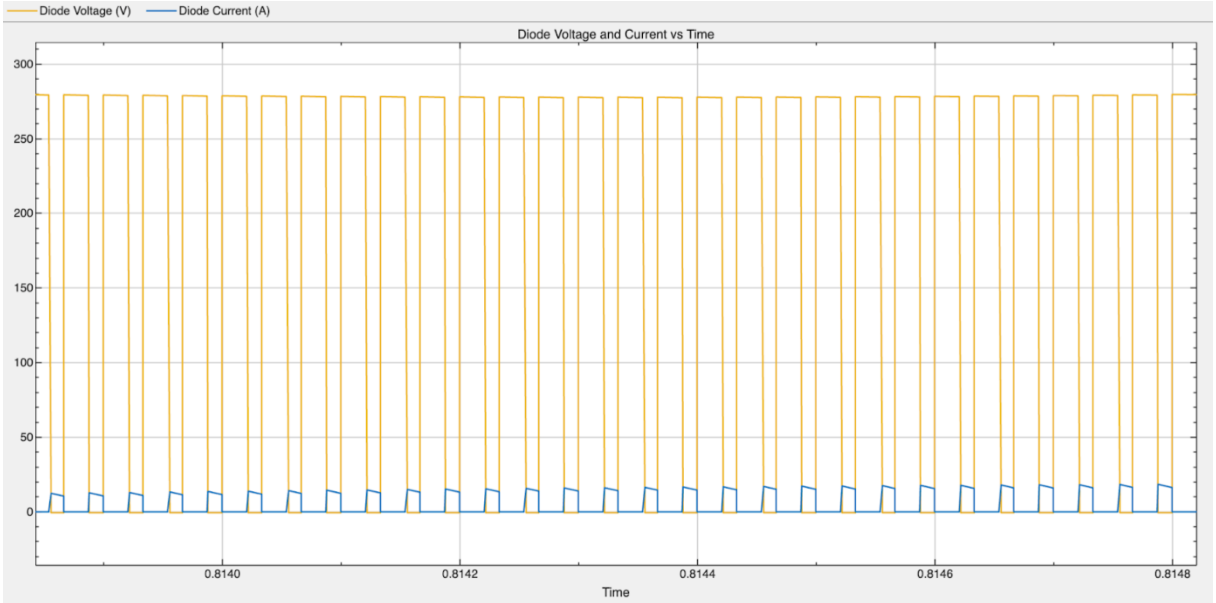

Figure 7: Diode Voltage & Current Waveforms

The freewheeling diode operates inversely to the switch, conducting only when the MOSFET is blocking. When the diode is forward-biased, it creates a path for the inductive current to flow, preventing the voltage build-up over the switch. In the blocking state, the diode shows no signs of conduction, correctly blocking the 280 V, as can be seen in the related graph, and the turn-on voltage is quite close to 0.

The switching MOSFET and the freewheeling diode are hence working complementarily, with one conducting when the other is blocking. This intended synchronization keeps the converter in continuous conduction mode (CCM) and prevents timing overlaps or soaring currents.

Component Selection

This project requires a good selection of components to handle the high voltage and current. To ensure material and human safety, it is crucial to choose proper components. Also, to prevent inrush current and voltage that can damage the equipment and circuit, we implemented a soft-start algorithm that gradually increases the duty cycle of the gate drive PWM from 0 to 0.8 in 20 seconds. The switching components (MOSFET & DIODE) can operate within the safe limits because of the soft-start implementation.

Bridge Rectifier

Firstly, to convert AC grid voltage to DC, we need a bridge rectifier. We have decided to use the KBPC3510W single-phase bridge rectifier module. It has a 1000V maximum voltage and a 35A maximum current limit. Thanks to its electrical characteristics, we can safely drive the system. Also, its metal case allows us to mount a heatsink onto its chassis. During tests, the rectifier provided the DC output expectedly and maintained thermal stability.

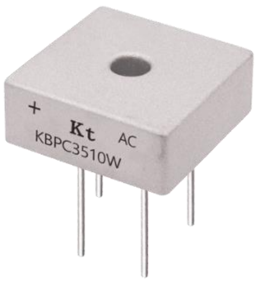

Figure 8: KBPC3510W Bridge Rectifier

Switching MOSFET

For the switching element of the buck converter, we selected the SPW47N60C3 (CoolMOS) power MOSFET. The main reason behind this selection is its high breakdown voltage rating, which is 650V. Despite the maximum theoretical voltage across the MOSFET being calculated as 325V (DC bus voltage), the stray inductances can cause high voltage spikes during switching. Hence, to ensure that the switch is operating within the safe limits, we decided to choose this MOSFET. Also, its 30A drain current rating allowed us to work within safe limits. With the low on-resistance, which is 0.07Ω, the power consumption is also reduced. We also ordered it in a TO-247 package to easily mount a large heatsink on it. This component also survived all tests without failure.

Figure 9: 47N60C3 MOSFET

Freewheeling Diode

At the planning stage, we chose our switching frequency as 30kHz. Because of this relatively high frequency, we decided to choose an ultrafast recovery diode. For this purpose, we have chosen the MUR3060 Ultrafast Recovery Diode. Its recovery time is approximately 60ns. Thus, we can use it in our 1kHz application without any change. Also, we ordered it in a TO-247 package to easily mount the heatsink.

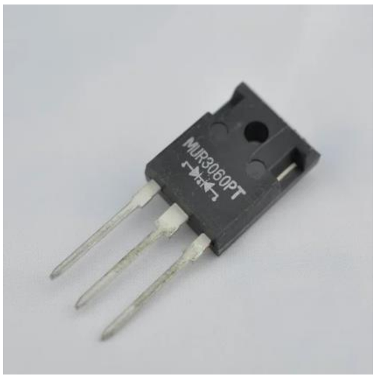

Figure 10: MUR3060 Diode

Gate Driver and Isolation Circuit

For the galvanic isolation, we decided to use a TLP250 Optocoupler between the control stage (Arduino Uno) and the power stage (Switching MOSFET). Thus, high transients and noises at the power stage do not affect the control stage. The Arduino PWM signal is 5V peak-to-peak, but our MOSFET gate-to-source voltage is about 8V. To solve this problem, we have forced to use a gate driver module.

This section is the most significant part of our implementation. At first, we attempted to use an IR2113 gate driver module with a classical buck driver topology. We have faced several problems in this design, such as the bootstrap circuit failing to feed the MOSFET, and the noise affected the system more than our expectations.

Figure 11: TLP250 Optocoupler

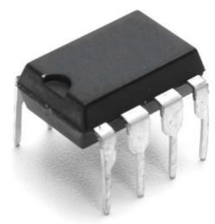

Figure 12: IR2106 Gate Driver

Then, we have decided to use a low-side switching topology to simplify the driving system. In this design, we used an IR2106 gate driver for our MOSFET gate drive. We also placed 100nF and 10µF by-pass capacitors across the supply pins and output pins to reduce the noise and stabilize the driver, and provide a better PWM signal.

Passive Components & Output Filtering

For the DC link at the primary side, we placed 2 470µF capacitors to reduce output ripple, and at the secondary side, we placed 3 100nF capacitors near the MOSFET to act as a snubber to ensure a low stray inductance. In the original buck converter design, there should be an LC filter at the output. We did not use an LC filter because of the inductance of the motor, which can be modeled as a huge inductor, and the capacitive effect of the back-emf. With the large inductance and capacitance of the motor, the buck converter operated in CCM and allowed us to reduce the size and the cost of the overall design.

Buck Converter Control

We used an Arduino Uno for our buck converter controller. With its internal timers, we can create exact PWM signals and implement a control algorithm. We couldn't implement a control structure because of the time and component-related problems. By using the features of the Arduino Uno, we implemented a soft-start algorithm to ensure that the current drawn by the motor is within the thermal limits. We used a gate driver to ensure that the MOSFET can draw the required current and voltage, and an optocoupler to ensure that high voltage and current transients on the power side do not affect the controller. The Arduino Uno can be seen in Figure 13.

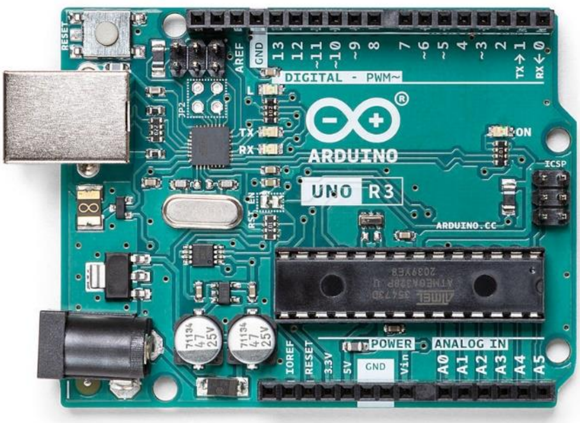

Figure 13: Arduino Uno

Loss Calculations

In this part, the loss calculations and the thermal analysis will be explained. To ensure that our components do not burn out or explode, we conducted a thermal analysis of the switching devices. The calculations in this section are made to demonstrate the worst-case scenario.

MOSFET Power Loss Analysis

The MOSFET is the main switching device in this design. With the low resistance of the selected MOSFET, it is relatively easy to handle thermal losses.

Table 4: MOSFET Datasheet Parameters (SPW47N60C3)

Parameter	Symbol	Value
Drain-Source On Resistance	$R_{DS,ON}$	0.07 Ω
Total Gate Charge	Q_G	50 nC
Max Junction Temperature	$T_{J(MAX)}$	150◦C

Conduction Losses

First, we found the effective current flowing through the switch. Since the duty cycle is 0.8:

$$I_{MOSFET,RMS} = I_{OUT} * \sqrt{D} = 12 * \sqrt{0.8} = 10.73A$$

Then we calculated the power loss using the resistance from the datasheet:

$$P_{cond} = I^2_{MOSFET,RMS} * R_{DS,ON} = 10.73^2 * 0.07 = 8.06W$$

We know that resistance goes up when the components get hot (as seen in Figure 14), but for this calculation, we used the standard value to keep it simple. So the overall conduction loss of the MOSFET is about 8W.

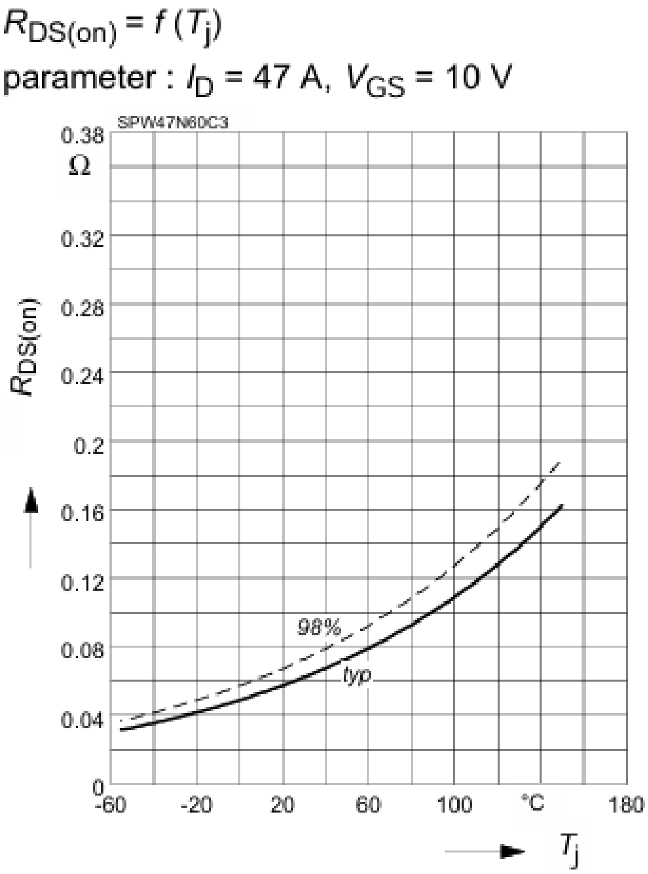

Figure 14: Variation of On-Resistance with Temperature (SPW47N60C3)

Switching Losses

Switching loss is the energy lost when the switch turns on and off. Since our frequency is very low (1 kHz), this loss is as small as possible. We estimated the switching time of the MOSFET to be 50 ns.

$$P_{SW} = 0.5 * V_{in} * I_{out} * t_{total} * f_{sw}$$

$$= (0.5) * (325V) * (12A) * (50 * 10^{-9}s) * (1000Hz) = 0.10W$$

As expected, switching losses are negligible compared to the conduction losses.

Hence, the total heat from the MOSFET is:

$$P_{MOSFET,TOTAL} = 8.06 + 0.10 = 8.16\,W$$

Diode Power Loss Analysis

For the diode, we used the MUR3060PT. It is a very fast diode, which is good for safety and efficiency. The important parameters of the MUR3060PT can be seen in Table 5.

Table 5: Diode Datasheet Parameters (MUR3060PT)

Parameter	Symbol	Value
Forward Voltage Drop	Vff	1.5 V
Reverse Recovery Time	trr	60 ns

Conduction Losses

The diode carries the current when the MOSFET is off.

$$I_{diode,avg} = I_{OUT} * (1 - D) = 12A \times 0.2 = 2.4\,A$$

From the graph in Figure 15, we see that the voltage drop is about 1.5 V.

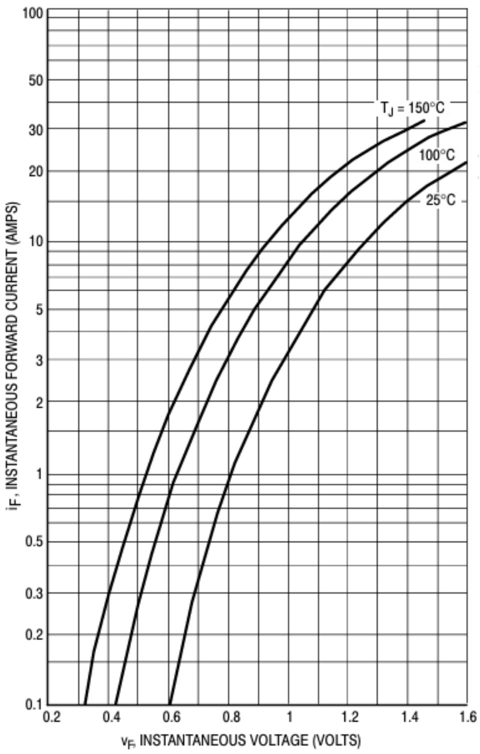

Figure 15: Forward Characteristics of the MUR3060PT Diode

$$P_{COND} = I_{diode\_avg} \times V_F = 2.4A \times 1.5V = 3.60\,W$$

Switching Losses

Even though it’s fast, it also has a minimal switching loss.

$$P_{SW} \approx 0.5 * V_{IN} * I_{RMS} * t_{rr} * f_{sw}$$

$$0.5 * 325V * 5A * (60 * 10^{-9}s) \times 1000Hz \approx 0.05\,W$$

Hence, the total diode loss is:

$$P_{Diode,TOTAL} = 3.60W + 0.05W = 3.65\,W$$

Thermal Verification

We used standard TO-247 heatsinks for cooling. These heatsinks have a thermal resistance of about 15 degrees Celsius per Watt if used without a fan. We also used thermal paste to help the heat go from the component to the heatsink.

First, we did a theoretical check to see what happens on paper.

TJ = TAMB +PLOSS × (RθJC +RθCH +RθHA)

TJ = 30+8.16 × (0.5+0.5+15) ≈ 160.6 ◦C

The calculation gave us 160.6 degrees Celsius. This was a problem because the maximum allowed is 150 degrees. It looked like passive cooling wouldn’t be enough. But we know that theoretical calculations assume the worst possible conditions, which don’t always reflect the situation in application.

To be sure, we tested it in the lab. We ran the motor driver at full load without a fan and watched the temperature with a thermal camera. In an expected way, the temperature only reached about 75 degrees Celsius after 5 minutes. At that point, we stopped the test.

We think the temperature stayed low for a couple of reasons. First, the motor didn’t draw the full 12 A continuously, like in our worst-case math. Second, since we built the circuit on a stripboard, we added very thick layers of solder on the power lines to carry the current. These thick solder tracks likely helped to spread the heat away from the MOSFET. Since 75 degrees is safe, we decided that we don’t need a fan.

Implementation

After figuring out how much power we would lose and carefully picking the parts, we moved on to the most important part of the project: building the hardware and making sure it worked. In this part, we show how we built the motor driver, talk about the big design changes we had to make to the gate driver circuit after several tries, and look at the waveforms we recorded during the tests.

We implemented the design on two 10x10cm stripboards. We ensured an enough distance for arcing and kept the components as close as possible to prevent stray inductances. We also used three separate heatsinks for the bridge rectifier, switching MOSFET, and freewheeling diode. We soldered the components to ensure electrical connection and physical stability.

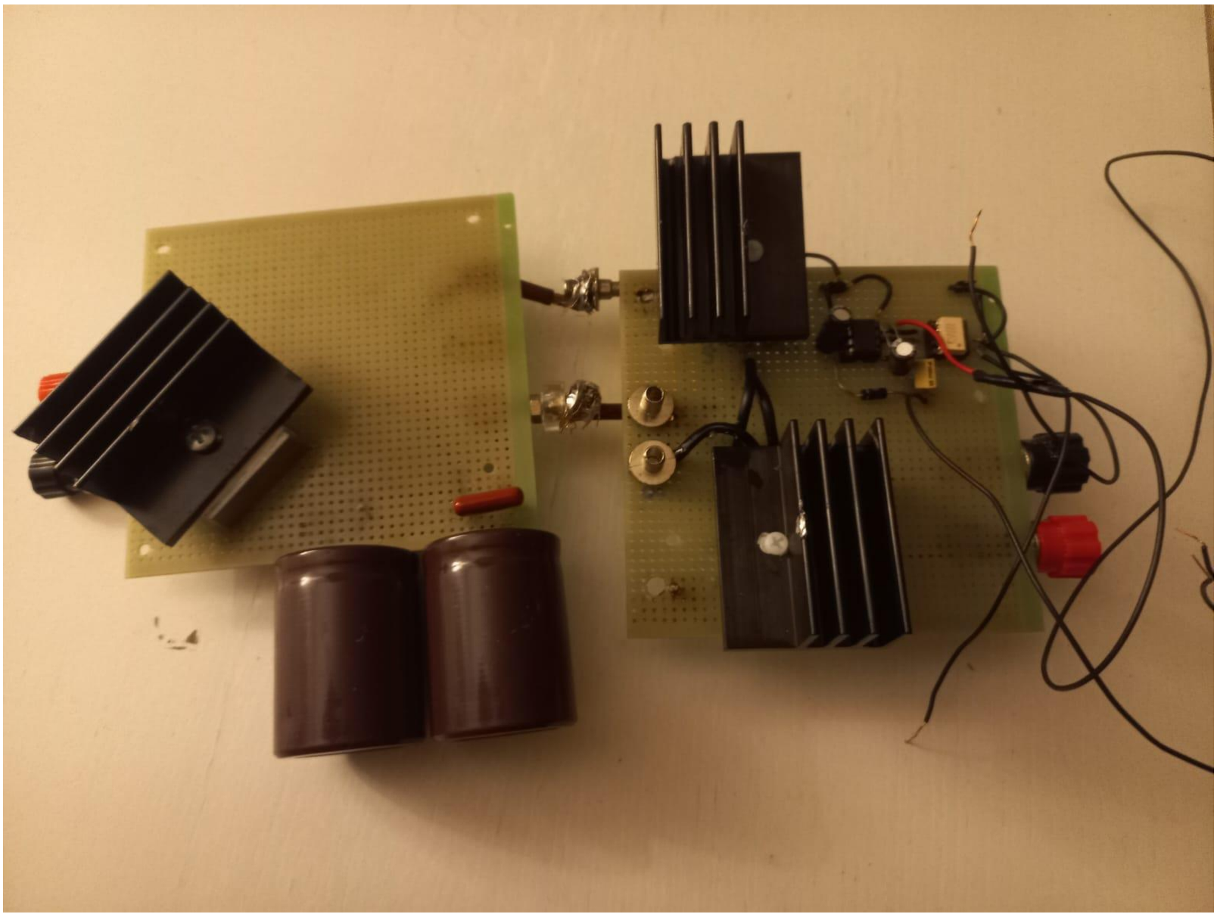

Figure 16: Overall Design Structure

Pre-Demo Test Results

In the rectifier stage, we used a 10x10 stripboard instead of making a custom PCB because we wanted to keep the prototype strictly experimental and flexible. But as we talked about in the thermal analysis section, we can't only use solder for electrical connection because there will be a high (10A) current on these paths. Hence, we have used AWG 14 for the connection. Thus, the high-power paths are strengthened against the high current. With this small change, we ensured that none of the joints face the overcurrent and hence overheating.

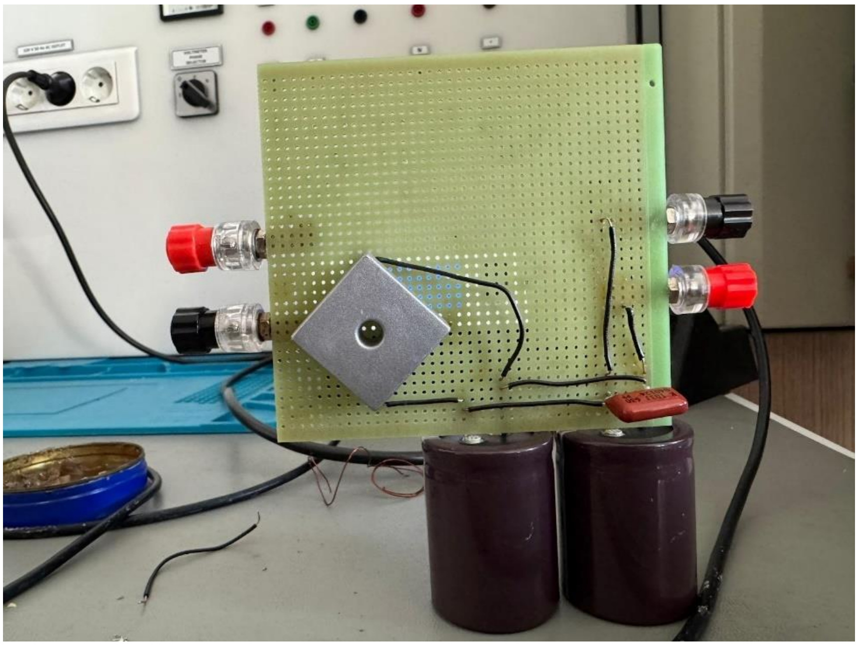

Figure 17: Physical Implementation of the Rectifier Stage on Stripboard

In Figure 17, we can see two 470nF output capacitors and a KBPC3510W bridge rectifier attached to the stripboard. We used a variac to test the system with a resistor load. When we turned on the variac gradually, we saw 300V average DC voltage with a 70V peak-to-peak swing. These are the expected results. We also waited until the capacitor discharged by measuring it before we touched the system.

The hardest part of this project was driving the MOSFET. We have tried several components and topologies before reaching success. First, we started with an IR2113 gate driver with a classical buck converter topology. The IR2113 driver requires a bootstrap circuit for high-gate drive. However, we could not achieve a high gate signal from the IC. Then we decided to use another gate driver IC. We do not know the exact reason of this malfunction, but we guess that the stray inductances can cause the stray inductances that can cause a malfunction.

We decided to change the gate driver and continue with the IR2106 gate driver with the same topology. The outcome of this topology was also the same. Thus, we decided that using a high-side MOSFET topology on the stripboard is not a good idea. Then we switched to the low-side MOSFET buck converter topology. We used IR2106 to drive low side MOSFET and succeeded this time. Because the MOSFET source and gate driver share the same ground, it is easier to implement this topology. Also, we did not use a bootstrap circuit. When we measure the gate signal, we saw that we have the intended PWM signal on the gate.

After solving the gate drive problem, we continued with the buck converter. To confirm that the optocoupler and gate driver work decently, we held a test on the buck converter. We measured the PWM signal of Arduino and the PWM signal at the output of the gate driver. We saw that our control stage works properly. The PWM signal of Arduino (blue line) and the PWM signal of the gate driver output (yellow line) can be seen in Figure 18. Note that the scales of the two measurements are different.

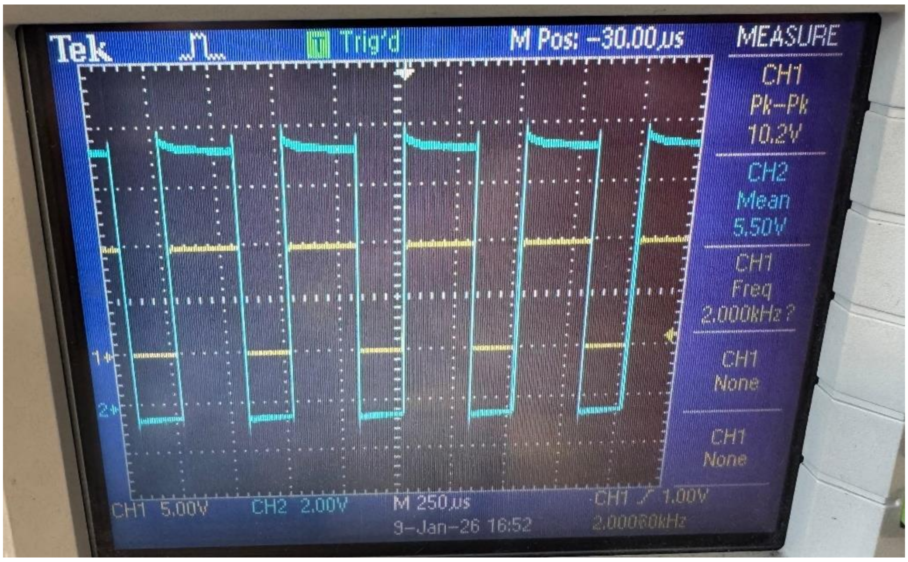

Figure 18: The PWM signal of Arduino (blue) and the PWM signal at the output of the gate driver (yellow).

Then, we tested the overall design with the resistor load and measured the output voltage and the thermal performance. The test rig can be seen in Figure 19. Note that the design changed after this test.

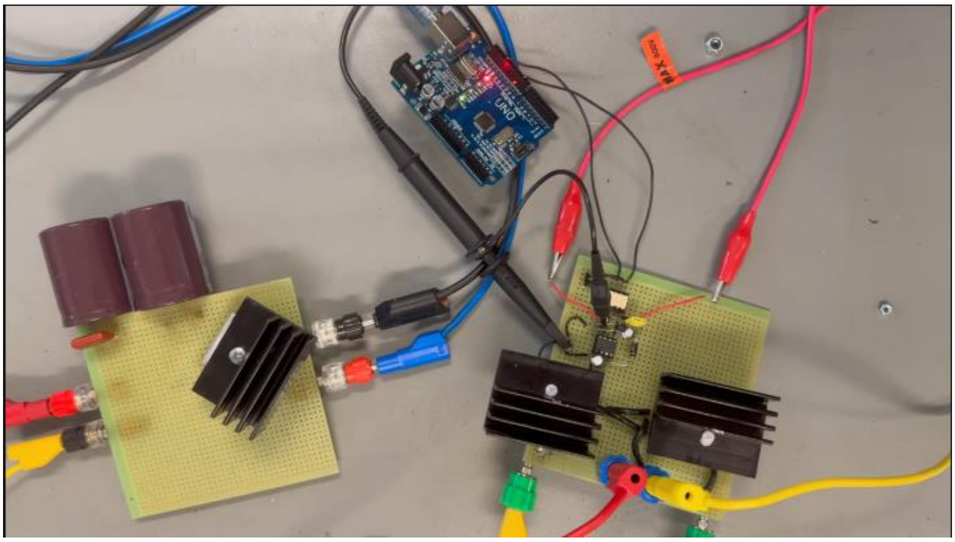

Figure 19: The Test Structure we used for the Overall Test.

Then we measured the output voltage with a multimeter and went up until we saw a 180V output with a 0.8 duty cycle. We left the system working for 10 minutes and did not encounter any thermal malfunction.

Demo Test Results

In the demo day, first, we held the resistor load test that we did before. There was no problem in this test. Then, we used our soft-start algorithm to run the DC motor. We made the connections and ran the motor. We did not encounter any problem while the motor was running on no-load. Then we moved on with the tea-bonus part. With a load, the motor started to draw much more current, and the thermal limits of the design were tested. The measurements on demo day can be seen in Figures 20, 21, 22, and 23.

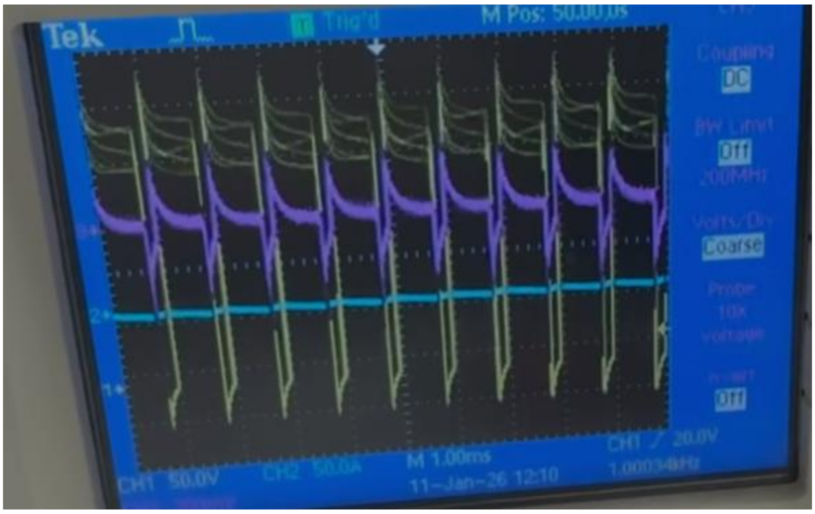

Figure 20: Steady-state no-load measurements for the motor at no load. Yellow is the output voltage, and purple is the output current.

Figure 21: Wattmeter Measurement for tea-bonus part

Figure 22: Multimeter measurement of Output Voltage for tea-bonus part

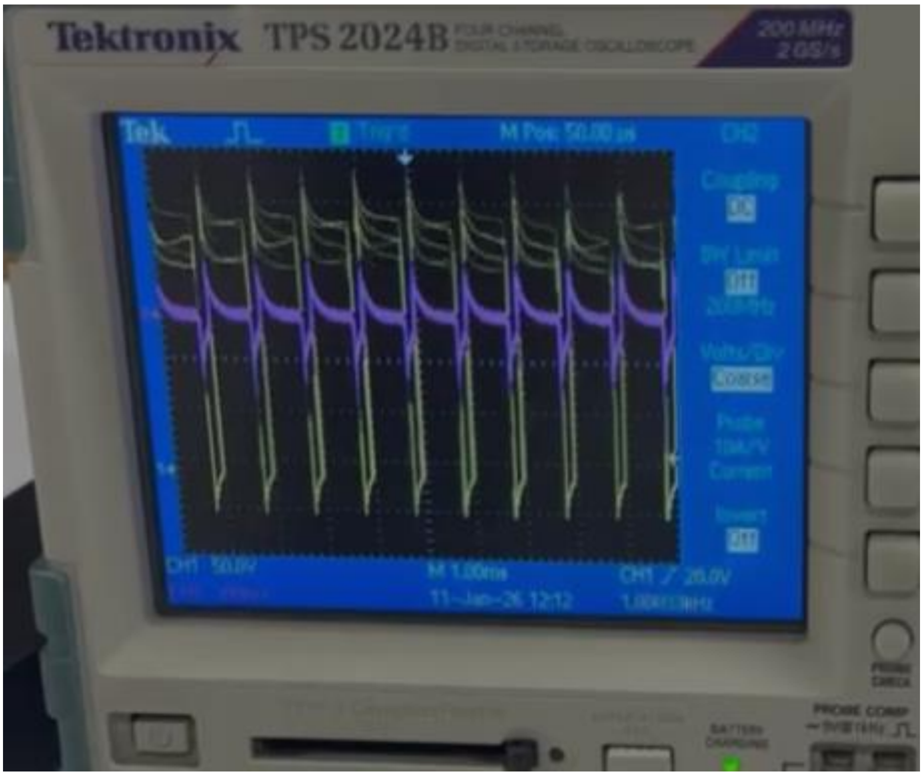

Figure 23: The Output voltage (yellow) and Output Current Waveforms for the tea-bonus part.

Note that, because of the 2-wattmeter connection used, the DC output voltage seems to be halved in the wattmeter measurement in Figure 21. The true output voltage measurement can be seen in the multimeter in Figure 22. The output current is kept constant at 175V at full load, and the output current is about 7.7-7.9A. The input power is measured as 1470.0W, and the output voltage is measured as 1358.6W, which can be seen in Figure 21. The tea-bonus part was successful with a 92.42% efficiency. Also, we reached the 180V output voltage, which is the maximum value required.

Thermal Results

In Figures 24 and 25, we can see the bridge rectifier and MOSFET final temperatures. The final temperature of the MOSFET is 73.7 degrees Celcius, the final temperature of the rectifier is 67.8 degrees. We can see that neither component achieved its thermal stability. Note that the diode remained about 40 degrees during operation, so we did not put it in the report.

Figure 24: Diode bridge final temperature.

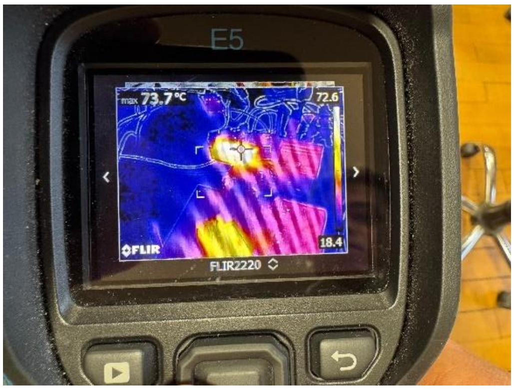

Figure 25: MOSFET final temperature.

Conclusion

In conclusion, the overall design succeed to achieve the requirements and drive the 2kW DC motor. The minimum requirements are achieved. By selecting the back-to-back single-phase diode rectifier and buck converter topology, we have achieved a balance between the power rating requirements, cost, and implementation simplicity.

Some of the key performance metrics of the overall design are:

- High Efficiency: The system reached about 92.42% of efficiency during the operation.
- Target Voltage Achievement: The motor driver module reached 180V of output voltage successfully.
- Effective Inrush Protection: The system ensured component safety during operation with a successful soft-start.
- Thermal Limits: The components stayed within the thermal limits due to correct calculations and cooling.

Design Iterations and Final Configuration

The most critical change during the implementation phase was the transition from the high-gate topology to the low-gate topology. This decision allowed the system to simplify the driving and eliminated the need for the bootstrap circuit. Thus, we had to abandon the closed-loop control to achieve a much healthier driving structure. Also, we used the motor's inherent inductance and capacitance to filter out the output voltage, and with this large inductor and capacitor, the motor is guaranteed to stay in continuous conduction mode operation. Also, the tea bonus was successful. This shows us the system is a reliable and efficient solution.

References

[1] Kingtronics, "KBPC35005W-KBPC3510W single phase bridge rectifiers," kingtronics.com. [Online]. Available: https://www.kingtronics.com/SinglePhase/kbpc35005w-kbpc3510w-bridge-rectifiers-kingtronics.

[2] SEE Institute Delhi, "47N60 C3 MOSFET," seeinstitutedelhi.com. [Online]. Available: https://seeinstitutedelhi.com/product/47n60-c3-mosfet/.

[3] IndiaMART, "MUR3060 ultra fast recovery rectifier," indiamart.com. [Online]. Available: https://www.indiamart.com/proddetail/mur3060-27153208312.html.

[4] Karaköy Elektronik, "IR2106 high and low side driver," karakoyelektronik.com. [Online]. Available: https://karakoyelektronik.com/guc-surucu-ve-yonetim-entegreleri/ir2106-23799.

[5] Kartal Otomasyon, "TLP250 photocoupler (GaAlAs Ired & photo-IC)," https://www.google.com/search?q=kartalotomasyon.com.tr. [Online]. Available: https://www.kartalotomasyon.com.tr/urun/tlp250-entegre.